SUPPORTING INFORMATION

Two-dimensional Fluorinated Boron Sheets: Mechanical, Electronic, and Thermal Properties

Rengin Peköz,[†] Mine Konuk,[‡] M. Emin Kilic,[‡] and Engin Durgun[*,‡]

Department of Electrical and Electronics Engineering, Atılım University, 06836 Ankara, Turkey, and UNAM - Institute of Materials Science and Nanotechnology, Bilkent University, Ankara 06800, Turkey

E-mail: durgun@unam.bilkent.edu.tr

[*]To whom correspondence should be addressed

[†]Department of Electrical and Electronics Engineering, Atılım University, 06836 Ankara, Turkey

[‡]UNAM - Institute of Materials Science and Nanotechnology, Bilkent University, Ankara 06800, Turkey

1. Adsorption Sites of single F Atom Adsorbed on Borophene

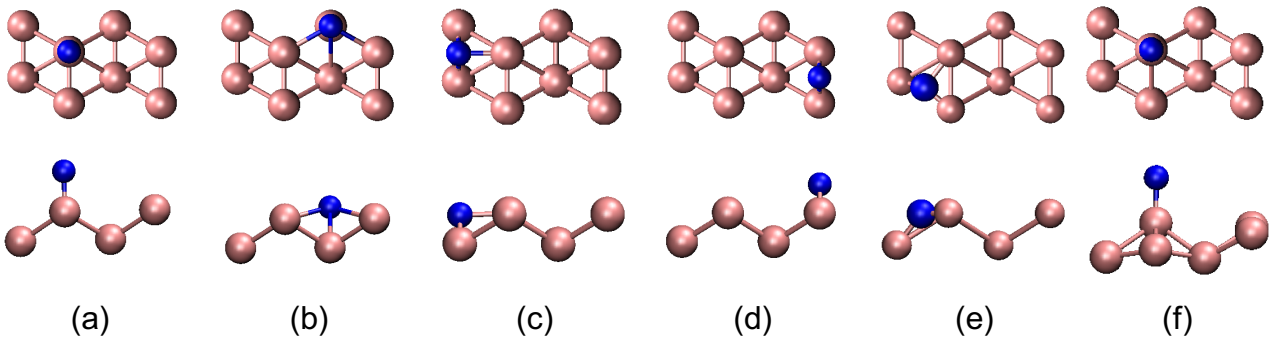

Figure S1: Schematic representation of (2x2) supercell of borophene showing F with various initial adsorption configurations: (a) F is on top site of upper B atom, (b) F is on top site of lower B atom, (c) F is on bridge site of lower B atoms, (d) F is on bridge site of upper B atoms, (e) F is on bridge site of lower and upper B atoms, and (f) the relaxed configuration of F adsorbed on borophene. B and F atoms are represented by pink and blue, respectively.

2. Adsorption Sites of two and four F Atoms Adsorbed on Borophene

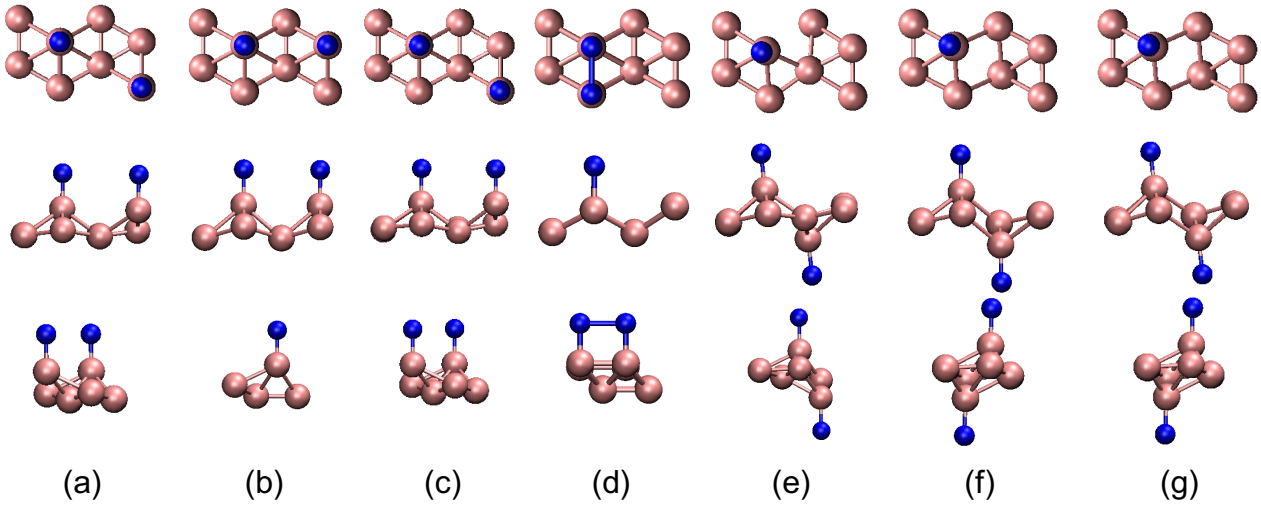

Figure S2: Schematic representation of (2x2) supercell of borophene showing two F atoms with various relaxed adsorption configurations. Single sided adsorptions: (a) F atoms are on top site of zigzag B, (b) F atoms are on top site of armchair B, (c) F atoms are on top site of row B, (d) F atoms are on top site of upper B and lower B, and double sided adsorptions: (e) F atoms are on top site of armchair B, (f) F atoms are on top site of upper B and lower B, and (g) F atoms are on top site of top zigzag B. Boron and F atoms are represented by pink and blue, respectively.

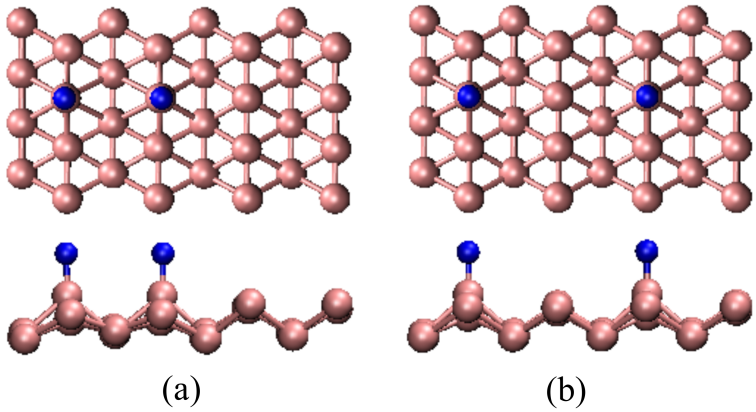

Figure S3: Schematic representation of (4x4) supercell of borophene showing two F atoms on the (a) adjacent and (b) second neighbor row boron atoms along the zigzag direction with relaxed adsorption configurations.

Table S1: Binding energy (E_b in eV/F) and structural parameters such as buckling height (h in Å) calculated for single and two F atoms on borophene.

System	E_b	d_{B-F}	h
Fig. 1(f)	**5.42**	1.37	1.20
Fig. 2(a)	5.02		
Fig. 2(b)	**5.30**	1.35	1.22
Fig. 2(c)	5.02		
Fig. 2(d)	1.40		
Fig. 2(e)	5.29		
Fig. 2(f)	5.29		
Fig. 2(g)	5.29		
Fig. 3(a)	**5.15**	1.36	1.13
Fig. 3(b)	4.91		
Fig. 4(a)	5.12		
Fig. 4(b)	**5.20**	1.36	1.31
Fig. 5(a)	1.32	1.54	0.82
Fig. 5(b)	unstable		
Fig. 6(a)	unstable		
Fig. 6(b)	1.20	2.22	0.72
Fig. 6(c)	unstable		

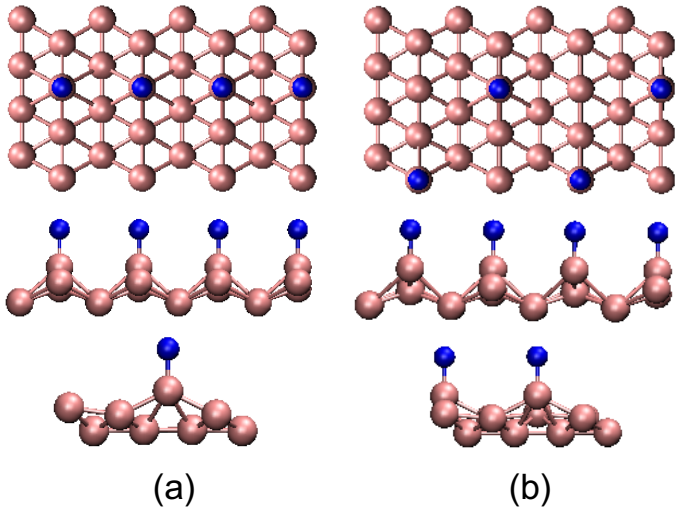

Figure S4: Schematic representation of (4x4) supercell of borophene showing four F atoms with linear and zigzag relaxed adsorption configurations along the zigzag direction. B and F atoms are represented by pink and blue, respectively.

3. Possible configurations for B_2F: Half coverage

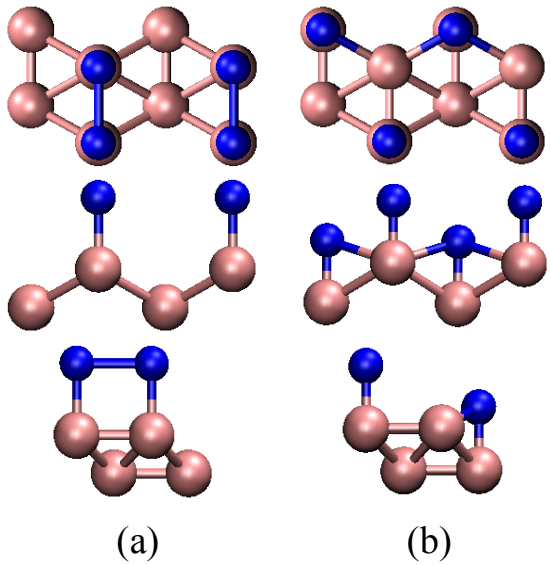

Figure S5: Schematic representation of (2x2) supercell of borophene showing the initial configurations for single side fluorination (B_2F(s)). B and F atoms are represented by pink and blue, respectively.

4. Possible configurations for BF: Full coverage

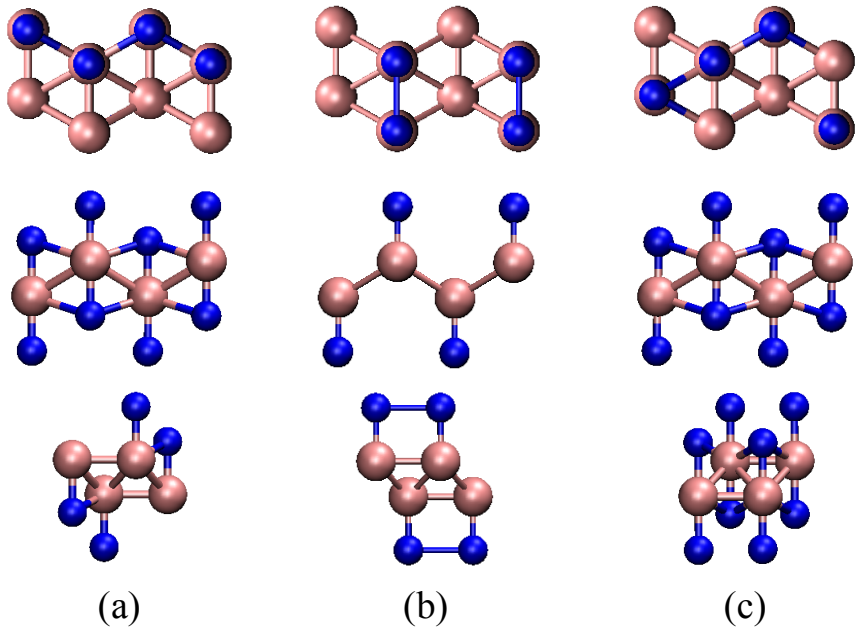

Figure S6: Schematic representation of (2x2) supercell of borophene showing the initial configuration for 100% coverage of fluorination (BF). B and F atoms are represented by pink and blue, respectively.

5. Structural Phase Transition of BF

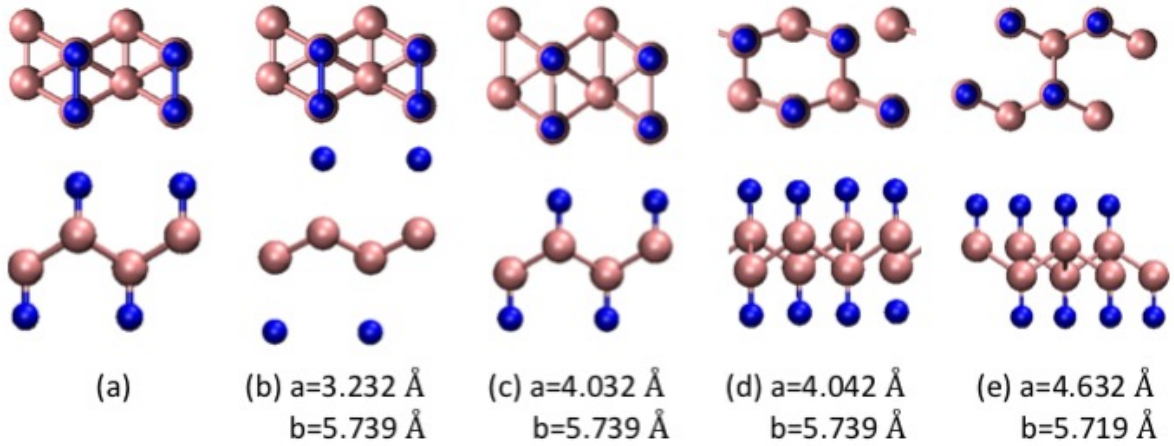

Figure S7: Schematic representation of (2x2) supercell of borophene showing configurations for 100% coverage of fluorination (BF(d)). a) Initial configuration, (b) the unstable configuration with the lattice constants used in this work, (c-d) the relaxed configurations with larger unit cell parameters exhibiting a phase transition in borophene, (e) the most energetic configuration with the phase transition

6. Unstable Configurations of B_2F

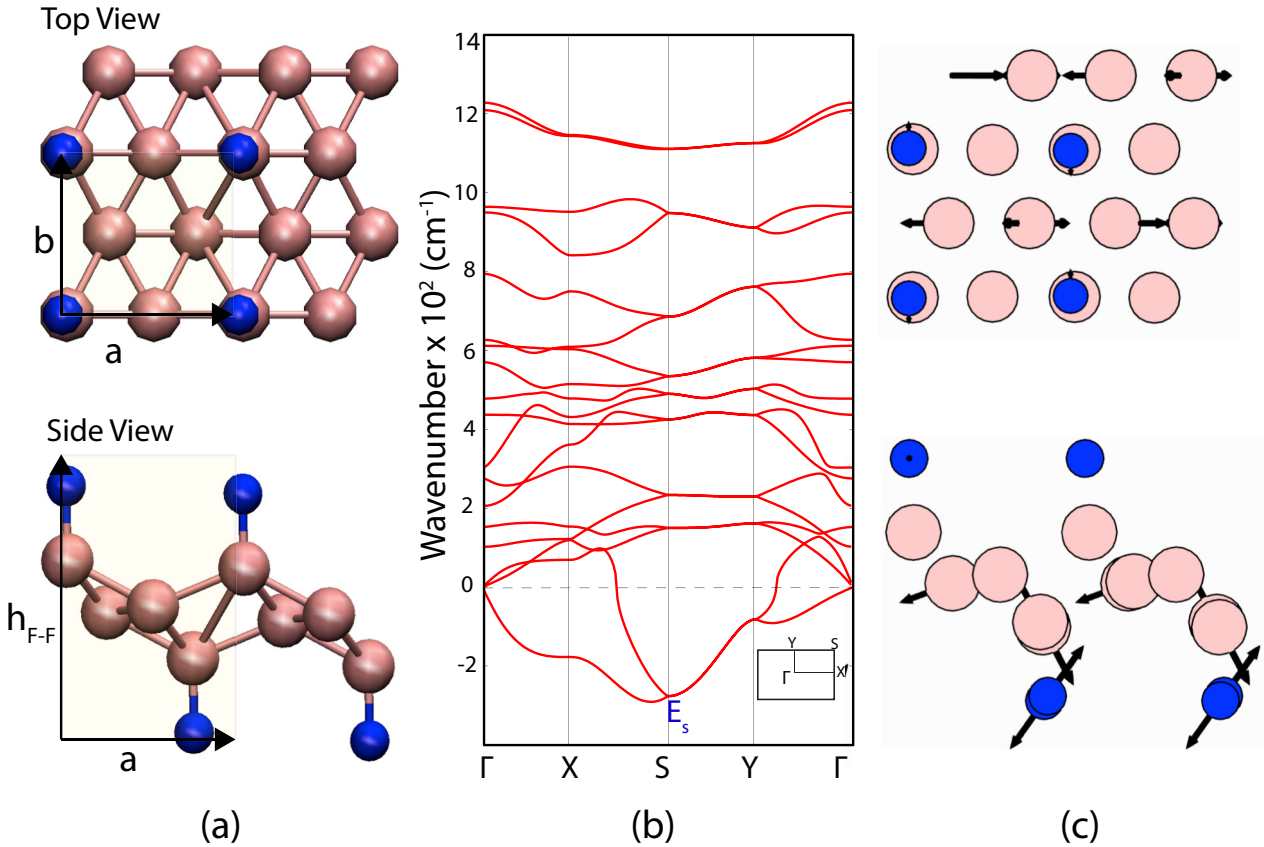

Figure S8: (a) Top and side view of double-sided fluorination of borophene, B_2F(d). The unit cell lattice vectors (a = 3.21 Å and b = 2.92 Å), height (h_{F-F} = 4.2 Å) are also shown. Although this structure is energetically one of the stable fluorinated borophene (E_b= 4.90 eV/F), the nature of phonons confirms that it is not a stable structure. (b) The imaginary frequency modes in phonon dispersion indicate that structure are dynamically unstable. (c) Eigenvector corresponding to the soft mode frequency (E_S) at S-point. The occurrence of instability is manifested in the phonon spectrum of the distorted structure by negative vibration frequencies. Two F atoms in the same plane at the bottom vibrate out of the plane and displace to inverse directions. One of the cause of failure may due to the linear order of F atoms. In the following Figure, we also assume that such doped structures are possible to be stabilized by doping concentrations.

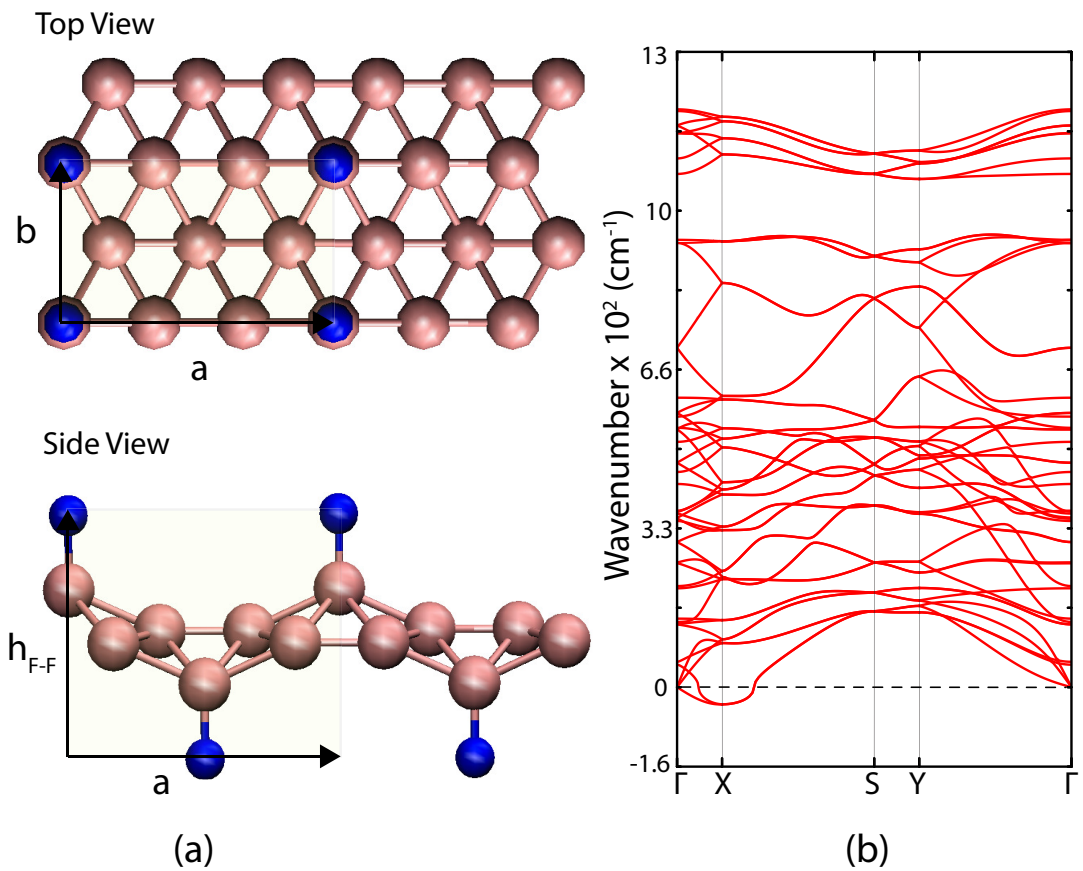

Figure S9: Unstable configuration of double-sided fluorination borophene with lower coverage: (a) Top and side view of double sided adsorptions. The unit cell lattice vectors (a = 9.83 Å and b = 2.90 Å) and height (h_{F-F} = 4.62 Å) are also shown. E_b of the system is 5.19 eV/F. (b) Softening in the spectra is indicative of the dynamical instability.

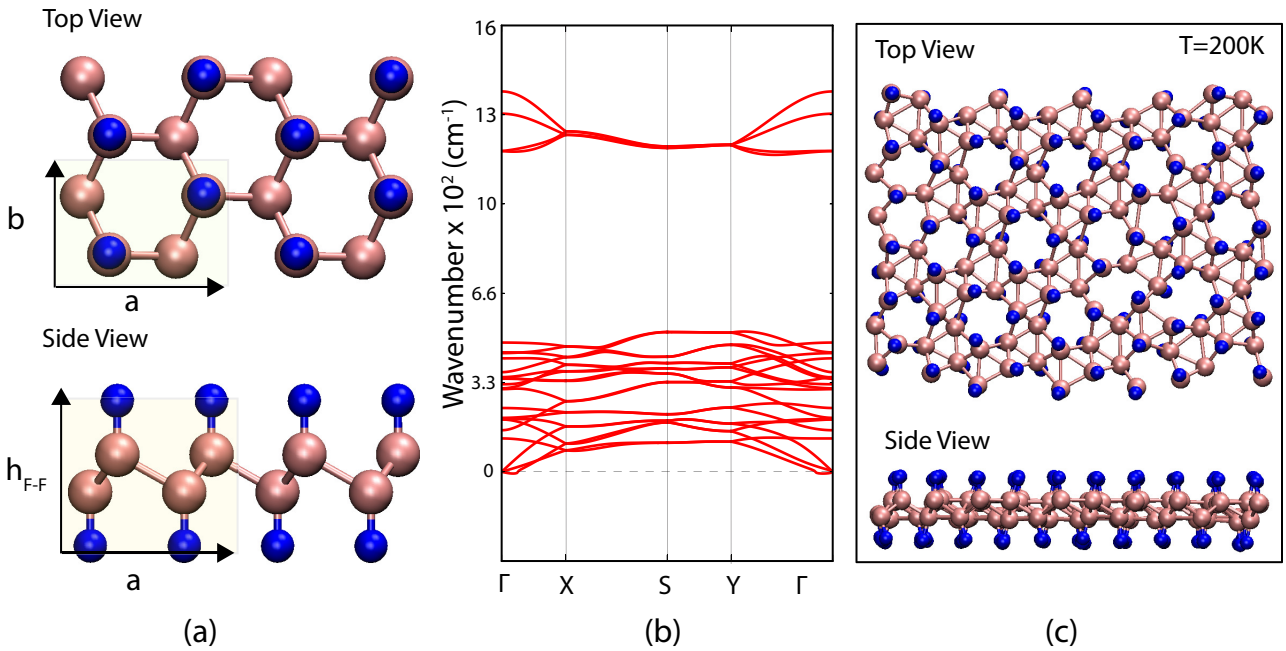

Figure S10: Full fluorination borophene (BF), hexagonal lattice: (a) Top and side view of borophene structure with full fluorination. The unit cell lattice vectors (a = 4.63 Å and b = 2.91 Å) and height (h_{F-F} = 3.57 Å) are also shown. (b) Small imaginary frequency is observed near Γ-point. (c) The snapshot of AIMD simulation. Phase transition occurs at 200 K and initial configuration of 100% coverage is not dynamically stable.

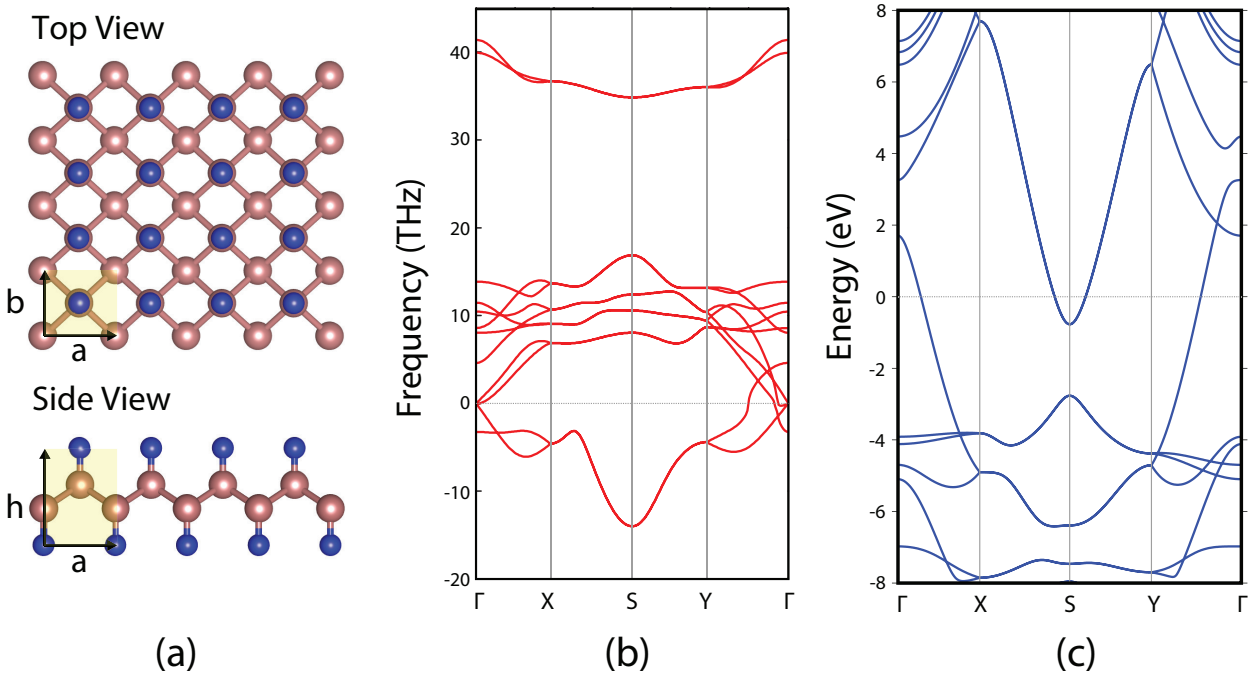

Figure S11: Full fluorination borophene (BF), rectangular lattice: (a) Top and side view of borophene structure with full fluorination. The unit cell lattice vectors (a = 5.11 Å and b = 4.76 Å) are also shown. (b) Phonon spectrum and (c) Electronic band structure of BF

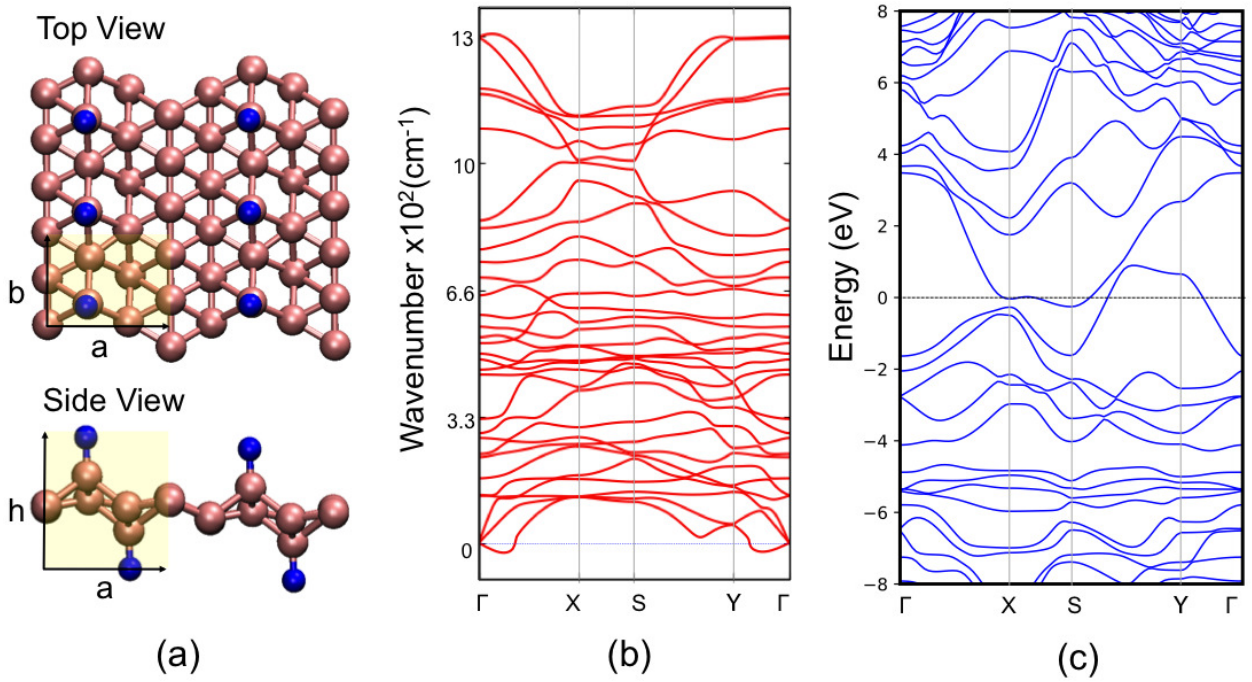

Figure S12: Double-sided fluorination with 25% coverage ($B_4F(d)$): (a) Top and side view of the structure. The unit cell lattice vectors (a = 3.25 Å and b = 5.78 Å) are also shown. (b) Phonon spectrum and (c) Electronic band structure of $B_4F(d)$

7. Mechanical Properties

Table S2: Calculated elastic constants (c_{ij}), shear modulus (G), Young's modulus (Y in N/m), and Poisson's ratio (ν) of bare, half (B_4F) and fully (B_2F) fluorinated borophene. References for bare borophene,[2] hydrogenated borophene (BH),[2] bare graphene,[3] and hydrogenated graphene (CH)[4] are tabulated as well.

Configurations	c_{11}	c_{22}	c_{12}	c_{66}=G	Y_a	Y_b	ν_a	ν_b
Borophene	376.60	149.60	-7.64	83.61	376.21	149.45	-0.051	-0.020
Borophene[1]	398.00	170.00	-7.00	94.00	398.00	170.00	-0.040	-0.020
Borophene[2]	379.00	162.50	-2.00	87.00	378.97	162.49	-0.012	-0.005
Graphene[3]	358.10	358.10	60.40	148.90	347.91	347.91	0.169	0.169
B_4F(s)	275.06	183.66	13.07	79.63	274.13	183.04	0.071	0.047
B_2F(d)	130.12	200.76	6.17	57.35	129.93	200.46	0.030	0.047
BH[2]	175.77	112.86	19.97	28.46	172.24	110.59	0.177	0.114
CH[4]	248.20		19.40		246.70	246.70	0.078	0.078

8. Thermal Properties

Helmholtz free energy (F), specific heat at constant volume C_V and entropy (S) can be expressed as[5]

$$F = -k_B T \ln Z = \frac{1}{2}\sum_{q_j} \hbar\omega_{q_j} + k_B T \sum_{q_j} \ln[1 - \exp(-\hbar\omega_{q_j}/k_B T)] \tag{1}$$

$$C_V = \left(\frac{\partial E}{\partial T}\right)_V = \sum_{q_j} k_B \left(\frac{\hbar\omega_{q_j}}{k_B T}\right)^2 \frac{\exp(\hbar\omega_{q_j}/k_B T)}{[\exp(\hbar\omega_{q_j}/k_B T - 1]^2} \tag{2}$$

$$S = \frac{\partial F}{\partial T} = \frac{1}{2T}\sum_{q_j} \hbar\omega_{q_j} \coth[\hbar\omega_{q_j}/2k_B T] - k_B \sum_{q_j} \ln[2\sinh(\hbar\omega_{q_j}/2k_B T) \tag{3}$$

where Z is the partition function, ω_{q_j} is the phonon frequency with the phonon mode index j and phonon wave vector, q.

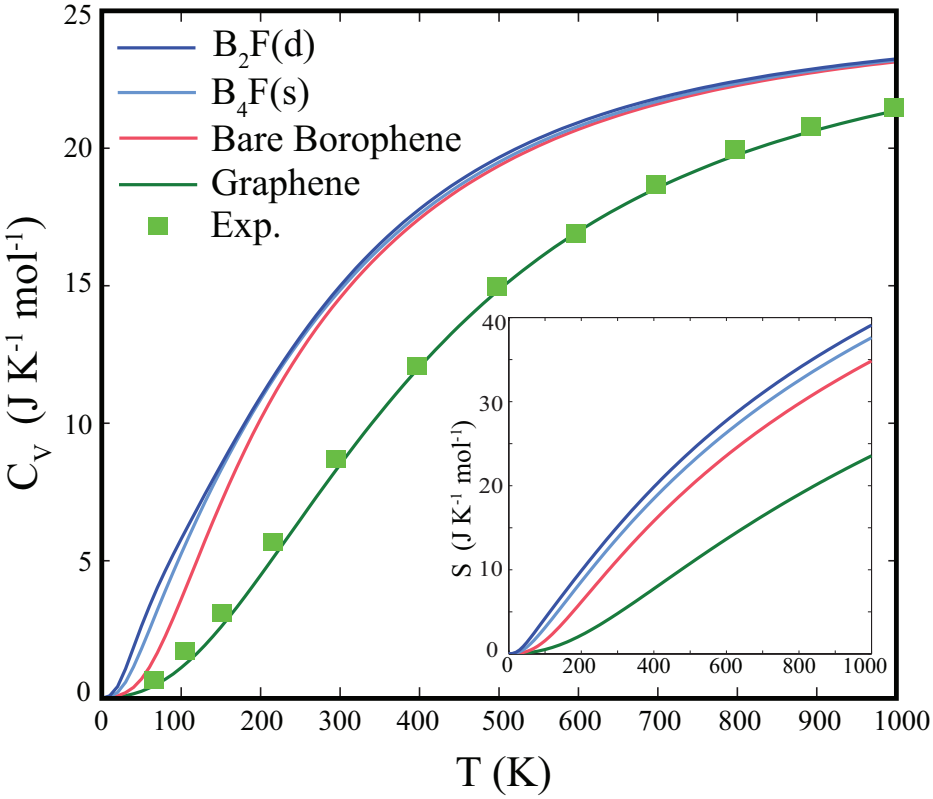

Figure S13: C_V of pure graphene at various temperatures compared with experiment is given for the sake of comparison[6]. The inset also indicates the variation of entropy (S).

References

(1) Mannix, A. J. et al. Synthesis of borophenes: Anisotropic, two-dimensional boron polymorphs. *Science* **2015**, *350*, 1513–1516.

(2) Wang, Z.; Lu, T.-Y.; Wang, H.-Q.; Feng, Y. P.; Zheng, J.-C. High anisotropy of fully hydrogenated borophene. *Phys. Chem. Chem. Phys.* **2016**, *18*, 31424–31430.

(3) Wei, X.; Fragneaud, B.; Marianetti, C. A.; Kysar, J. W. Nonlinear elastic behavior of graphene: Ab initio calculations to continuum description. *Phys. Rev. B* **2009**, *80*, 205407.

(4) Peng, Q.; Liang, C.; Ji, W.; De, S. A theoretical analysis of the effect of the hydrogenation of graphene to graphane on its mechanical properties. *Phys. Chem. Chem. Phys.* **2013**, *15*, 2003–2011.

(5) Togo, A.; Chaput, L.; Tanaka, I.; Hug, G. First-principles phonon calculations of thermal expansion in Ti3SiC2, Ti3AlC2, and Ti3GeC. *Phys. Rev. B* **2013**, *87*, 174301.

(6) Pop, E.; Varshney, V.; Roy, A. K. Thermal properties of graphene: Fundamentals and applications. *MRS Bull.* **2012**, *37*, 1271.